ELSEVIER

Spectrochimica Acta Part A 58 (2002) 3167–3178

SPECTROCHIMICA
ACTA
PART A

www.elsevier.com/locate/saa

Thermal and kinetic studies on solid complexes of 2-(2-benzimidazolylazo)-4-acetamidophenol with some transition metals

G.G. Mohamed *, M.A. Zayed, Nadia E.A. El-Gamel

Chemistry Department, Faculty of Science, Cairo University, Giza, Egypt

Received 12 February 2002; accepted 21 February 2002

Abstract

The preparation and characterization of 2-(2-benzimidazolylazo)-4-acetamidophenol (BIAAP) complexes are reported. Different physico-chemical methods like IR, Magnetic, solid reflectance spectra and molar conductance, were used to investigate the structure of BIAAP complexes. In particular, the thermal decomposition of Fe(III), Co(II), Ni(II), Cu(II), Zn(II) and Cd(II) complexes of BIAAP is studied in nitrogen atmosphere. All the complexes do not contain coordinated water molecules but contain (2–4) water molecules of crystallization. The water molecules were removed in a single step. The complexes of Co(II) and Ni(II) ions exhibited a phase transition and the decomposition or combustion of BIAAP occurred in the second and subsequent steps. The final decomposition products were identified by mass spectrometry as the corresponding metal oxides or carbonate. The activation thermodynamic parameters, such as, energy of activation, enthalpy, entropy and free energy change of the complexes were evaluated and the stabilities of the thermal decomposition of the complexes are discussed. From the kinetic point of view, it is found that the thermal stability of the complexes follows the order Ni(II) > Cu(II) > Zn(II) > Fe(III) > Co(II) > Cd(II).

Keywords: TG and DTA; 2-(2-Benzimidazolylazo)-4-acetamidophenol complexes; IR; Conductance; Solid reflectance; Mass spectrometry

---

1. Introduction

Argoud et al. [1] used 2-aminobenzimidazole and other benzimidazole derivatives as a complexing agent in the purification of water from heavy metals. Ihara et al. [2] prepared a square planar Ni(II) complexes with 2-aminobenzimidazole and investigated their thermal transformation into octahedral structure in the solid phase. $Cu(OAc)_2L$ and $Cu(OAc)_2L_2$ (L = 2-aminoimidazole, 2-aminobenzimidazole) were prepared and characterized by IR spectra. The decrease in the NH_2 group vibrational frequency was attributed to the inter- or intra-molecular H-bonding [3]. Co(II) and Fe(III) complexes with 2-substituted benzimidazole derivatives were prepared and characterized by spectroscopic and magnetic measurements [4].

---

* Corresponding author. Fax: +20-202-572556

E-mail address: ggenidy@hotmail.com (G.G. Mohamed).

1386-1425/02/$ - see front matter © 2002 Published by Elsevier Science B.V.
PII: S1386-1425(02)00122-1

A comparative study on the stability and extractability of Co(II), Ni(II), Cu(II) and Cd(II) complexes of benzimidazole, 2-aminobenzimidazole and 2-methylbenzimidazole was done by Lenarcik et al. [5]. The reaction of $FeCl_2$ with some 2-aminobenzimidazole ligands yield monomeric and dimeric $[Fe(L)Cl_2]$ complexes. These complexes were characterized by different tools of analyses and found to have a pseudotetrahedral structure [6–8].

The preparation and thermal characterization (TG and DTA) of the transition metal complexes of this new azo compound, 2-(2-benzimidazolylazo)-4-acetamidophenol (BIAAP), have not been reported earlier. The literature survey, concerning the thermal behaviour of this ligand and its complexes are scantly. Therefore, the present work aimed chiefly to through more light on thermal behaviour of BIAAP complexes of di- and tri-valent transition metal ions. Scheme representing the thermal decomposition of these metal complexes was suggested. Different activation thermodynamic data are calculated from the DTG curve and correlated qualitatively and quantitatively with the atomic radii of the different metal ions. The coordination behaviour of BIAAP towards different transition metals is reported using different analytical tools.

2. Experimental

2.1. Materials and methods

All chemicals used were of the analytical reagent grade. They included 4-acetamidophenol (Sigma), 2-aminobenzimidazole (Aldrich), sodium nitrite and hydroxide (BDH), ethyl alcohol (Adwic) and the disodium salt of ethylenediaminetetraacetic acid (Adwic). Cupric acetate dihydrate (Prolabo), cobalt and nickel chlorides hexahydrate (BDH), zinc chloride dihydrate and cadmium chloride (Adwic) and ferric chloride (Riedel-de Haën) were used as received. The elemental anlyses (C, H, N) were made at the Microanalytical Center at Cairo University. IR spectra were recorded on a Perkin-Elmer FT-IR type 1650 spectrophotometer. The solid reflectance spectra were measured on a Shimadzu 3101 PC spectrophotometer. The molar magnetic susceptibilities were measured on powdered samples using the Faraday method. The conductance measurements were carried out using a Sybron–Barnstead conductometer. A Shimadzu TGA-50H and DTA-50H thermal analyzers were used to record simultaneously TG, DTG and DTA curves. The experiments were carried out in dynamic nitrogen atmosphere (20 ml min^{-1}) with a heating rate of 10 °C min^{-1} in the temperature range 20–1000 °C using platinum crucibles. The sample sizes ranged in mass from 1.2 to 3.5 mg. Highly sintered α-Al_2O_3 was used as a reference. The mass spectra were recorded with EI technique at 70 eV on a Hewlett-Packard Model MS-5988 GS-MS instrument in the Microanalytical Center at Cairo University. Metal contents were determined by titration against standard EDTA after complete decomposition of the complexes with aqua regia in a Kjeldahl flask several times.

2.2. Synthesis of 2-(2-benzimidazolylazo)-4-acetamidophenol

2-Aminobenzimidazole (3.99 g, 100 mmol) was mixed with HCl (11.5 M, 5 ml) and diazotized below 5 °C with $NaNO_2$ (2.07 g, 10 mmol). The resulting diazonium chloride was coupled with an alcoholic NaOH (3 g, 25 ml) solution of 4-acetamidophenol (4.53 g, 10 mmol) below 5 °C. The product was separated by filtration, purified by crystallization from diethyl ether and dried in vacuo over anhydrous calcium chloride. The red azo product is produced in 70% yield with a m.p. = 160 °C.

2.3. Preparation of complexes

The metal complexes of BIAAP were prepared by the addition of the appropriate metal chloride or acetate solutions (0.01 mole) in ethanol–water mixture (1:1) to the solution of the azo compound (0.02 mole) in the same solvent (50 ml). The resulting mixture was stirred under reflux for one half-hour where upon the complexes were precipitated. They were collected by filtration, washed with 1:1 ethanol:water mixture and with diethylether. The general reaction for the preparation of the metal complexes of BIAAP is:

$$\text{MA} + 2\text{BIAAP} + x\text{H}_2\text{O} \Rightarrow [\text{M(BIAAP)}_2]x\text{H}_2\text{O}$$

where M = Fe(III), Co(II), Ni(II), Cu(II), Zn(II) and Cd(II), A = Cl in case of Co(II), Ni(II), Fe(III) and Cd(II) ions and OAc in case of Cu(II) and Zn(II) ions; and $x = 2$–4.

2.4. Kinetic analysis

The first stage of dehydration of the complexes was studied in detailed manner. The kinetic parameters such as activation energy (ΔE^*), enthalpy (ΔH^*), entropy (ΔS^*) and free energy change of the decomposition (ΔG^*) were evaluated graphically by employing the Coast–Redfern relation [9]:

$$\log\left[\frac{\log\{W_f/(W_f - W)\}}{T^2}\right] = \log\left[\frac{AR}{\theta E^*}\left(1 - \frac{2RT}{E^*}\right)\right] - \frac{E^*}{2.303RT} \quad (1)$$

where W_f is the mass loss at the completion of the reaction, W is the mass loss up to temperature T; R is the gas constant, E is the activation energy in kJ mol^{-1}, θ is the heating rate and $(1-(2RT/E^*)) \cong 1$. A plot of the left-hand side of Eq. (1) against $1/T$ gives a slope from which E^* was calculated and A (Arrhenius constant) was determined from the intercept. The entropy of activation (ΔS^*), enthalpy of activation (ΔH^*) and the free energy change of activation (ΔG^*) were calculated using the following equations:

$$\Delta S^* = 2.303[\log(Ah/kT)]R \quad (2)$$

$$\Delta H^* = E^* - RT \quad (3)$$

$$\Delta G^* = H^* - TS^* \quad (4)$$

where k and h are the Boltzman and Blanck constants, respectively. The calculated values of E^*, A, ΔS^*, ΔH^* and ΔG^* for the decomposition steps are given in Table 3.

3. Result and discussion

The results of the elemental analyses of BIAAP metal complexes are shown in Table 1. In all cases 1:2 (M:L) solid complexes are isolated and found to have the general formulae $[\text{ML}_2]\cdot x\text{H}_2\text{O}$ where M = Ni(II), Co(II), Cu(II), Zn(II) and Cd(II) or $[\text{ML}_2]\text{Cl}\cdot x\text{H}_2\text{O}$ where M = Fe(III), that is in agreement with the stoichiometric ratio found by the spectrophotometric methods. The DMF solubility of the complexes permitted calculation of the molar conductivity (Λ_m) of 10^{-3} M solution at 25 °C [10], and by comparison, the type of electrolyte of each complex. The molar conductivity value for Fe(III) complex is 104 ohm^{-1} cm^2 mol^{-1} indicating a 1:1 electrolyte and on the other hand, the low conductivity values of the remaining complexes prove their weak molecular nature (Table 1).

3.1. IR spectra and mode of bonding

The IR spectrum of the ligand shows a broad band at 3547 cm^{-1} due to νOH of the phenolic group. This band is absent in all the complexes indicating coordination through the deprotonated phenolic OH group [11]. The N=N stretching vibration is shifted to lower frequencies or even disappeared, hidden under other frequencies when the spectra of the free ligand is compared with those of the complexes. This indicates the involvement of the azo group in coordination to the metal ions [12]. The band at 1610 cm^{-1} due to the N3 imidazole nitrogen, could not be assigned in the Fe(III), Co(II) and Ni(II) complexes, while decrease in intensity in case of Cu(II) complex indicating that it has been affected upon coordination to the metal ions. But in case of Cd(II) and Zn(II) complexes, this band is not affected indicating the non-involvement of the N3 imidazole nitrogen in coordination to these metal ions [13]. In the far IR spectra of all the complexes, the bands observed at 515–573 cm^{-1} (M–N) and 414–432 cm^{-1} (M–O) provide conclusive evidence concerning the bonding of nitrogen and oxygen to the metal ions [11].

Table 1
Analytical and physical data of BIAAP and its metal complexes

Compound	Colour (% yield)	M.P. (°C)	Found (calcd.)%				Molecular wt. found (calcd.)	μ_{eff} (B.M.)	Conductance (Ω^{-1} cm^2 mol^{-1})
			C	H	N	M			
Ligand [H_3L]	Red	160	60.6	4.3	23.56		297	–	–
	(70)		(61)	(4.4)	(23.73)		(295)		
[$FeC_{30}H_{24}N_{10}O_4$]	Violet	> 300	49.7	4.5	19.23	7.7	718	4.15	104
$\cdot 2H_2O$	(73)		(50.3)	(4.2)	(19.56)	(7.82)	(715.5)		
[$CoC_{30}H_{24}N_{10}O_4$]	Dark green	> 300	52.45	4.1	20.08	8.29	680	5.2	16.7
$\cdot 2H_2O$	(80)		(52.7)	(4.3)	(20.49)	(8.63)	(683)		
[$NiC_{30}H_{24}N_{10}O_4$]	Greenish blue	> 300	50.2	4.45	19.21	8.00	722	3.1	16.1
$\cdot 4H_2O$	(67)		(50.06)	(4.7)	(19.47)	(8.2)	(719)		
[$CuC_{30}H_{24}N_{10}O_4$]	Light green	> 300	49.28	4.46	8.43	720		1.7	10.0
$\cdot 4H_2O$	(85)		(49.75)	(4.69)	(19.35)	(8.77)	(723.5)		
[$ZnC_{30}H_{24}N_{10}O_4$]	Blue	> 300	50.09	4.00	20.15	9.33	690	Diam.	16.7
$\cdot 2H_2O$	(75)		(50.24)	(4.3)	(20.32)	(9.43)	(689)		
[$CdC_{30}H_{24}N_{10}O_4$]	Reddish brown	> 300	47.2	3.8	18.34	15.54	737	Diam.	22.2
$\cdot 2H_2O$	(78)		(47.91)	(4.07)	(19.02)	(15.21)	(736)		

Table 2
Thermalanalytical results (TG, DTG, DTA) of the BIAAP–metal complexes

Complex	TG range (°C)	DTG_{max} (°C)	Peak temp in DTA (°C)	Estim (calc%)		Assignment
				Mass loss	Total mass loss	
$[FeC_{30}H_{24}N_{10}O_4]Cl\cdot 2H_2O$	50–202	80	60 (+)	10.09 (10.13)		Loss of two H_2O and one HCl molecules
	202–665	303	285 (−), 330 (+), 480 (+)	78.74 (78.68)	88.83 (88.81)	Loss of two ligand molecules and formation of $\frac{1}{2}$ Fe_2O_3
$[CoC_{30}H_{24}N_{10}O_4]\cdot 2H_2O$	50–205	49	90 (−)	5.07 (5.27)		Loss of two H_2O molecules
	205–650	447	360(−), 480(+), 570 (+)	83.72 (84.04)	88.79 (89.31)	Loss of two ligand molecules and formation of CoO
			770			Phase transition
$[NiC_{30}H_{24}N_{10}O_4]\cdot 4H_2O$	50–185	50	38 (+)	9.33 (10.01)		Loss of four H_2O molecules
	185–565	433	350 (−), 480 (−)	79.03 (79.55)	89.56 (88.36)	Loss of two ligand molecules and formation of NiO
			610			Phase transition
$[CuC_{30}H_{24}N_{10}O_4]\cdot 4H_2O$	50–205	55	30 (+), 60 (−)	5.39 (4.98)		Loss of two H_2O molecules
	205–770	471, 666	350 (−), 430(+)	77.95 (77.11)	82.5 (82.93)	Loss of two H_2O and ligand and formation of $CuCO_3$
			560 (+), 660 (+)			
$[ZnC_{30}H_{24}N_{10}O_4]\cdot 2H_2O$	50–215	52	100 (−)	7.49 (7.55)		Loss of two H_2O molecules and CH_4 gas
	215–460	335	280 (+), 400 (−)	19.25 (19.45)		Loss of $C_7H_4N_2O$ molecule
	460–955	723	500 (+), 600 (+) 680 (+), 900 (+)	60.45 (61.25)	87.19 (88.25)	Loss of ligand molecules and formation of ZnO
$[CdC_{30}H_{24}N_{10}O_4]\cdot 2H_2O$	50–190	74	130 (+)	6.26 (7.07)		Loss of two H_2O molecules and CH_4 gas
	190–275	237	200 (+), 250 (+)	4.82 (4.35)		Loss of CO and $2H_2$ gases
	275–490	376	400 (+), 460 (+)	19.65 (19.7)		Loss of $C_7H_3N_3O$, molecule
	490–1000	795	680 (+), 800(−), 920 (+)	51.68 (51.5)	82.41 (82.62)	Loss of ligand molecules and formation of CdO

(−) Exothermic, (+) endothermic.

3.2. *Magnetic susceptibility and electronic spectra measurements*

The solid reflectance spectra of the Cu(II) complex give band centered at 846 nm ($\mu_{eff} = 1.7$ B.M.), which may be assigned to $^2E_g \rightarrow {}^2T_{2g}$ transition in an approximately octahedral environment [11]. The magnetic moment of the Ni(II) complex has been found to be 3.1 B.M., which is within the range of values corresponding to octahedral geometry. The solid reflectance spectra of the Ni(II) complex are consistent with the formation of an octahedral geometry with the appearance of three bands at: ν_1 (456 nm): $^3A_{2g} \rightarrow {}^3T_{2g}$; ν_2: (714 nm): $^3A_{2g} \rightarrow {}^3T_{1g}$(F) and ν_3: (838 nm): $^3A_{2g} \rightarrow {}^3T_{1g}$(P). The 10Dq value of 838 nm confirm the octahedral configuration [14]. For the cobalt complex, the magnetic moment (5.2 B.M) is within the range of octahedral cobalt(II) complexes [11,14]. The solid reflectance spectrum shows three bands of medium intensity at 568, 754 and 842 nm which are assigned, respectively, to the transition $^4T_{1g}$(F)$\rightarrow {}^4T_{1g}$(P) (υ_3), $^4T_{1g}$ (F)$\rightarrow {}^4A_{2g}$ (F) (υ_2) and $^4T_{1g}$ (F)$\rightarrow {}^4T_{2g}$(F) (υ_1) of an octahedral cobalt(II) complex [14]. The magnetic moment of the iron(III) complex has been found to be 4.15 B.M., which is within the range of values corresponding to high-spin octahedral complexes of iron(III) ions. The zinc and cadmium complexes are diamagnetic and are likely to be tetrahedral.

3.3. *Thermogravimetric analysis*

The importance of this study on the BIAAP ligand and its complexes stems from their possible biological activities. Therefore, they are widely subjected to investigation by thermal analyses and other physico-chemical methods. Thermal data of the complexes are given in Table 2 and the activation thermodynamic data associated with the loss of water of crystallization (dehydration process) and ligand molecules are listed in Table 3. The previously reported data of microanalysis and mass spectra of the solid complexes give the general formula: $[MC_{30}H_{24}N_{10}O_4](A) \cdot xH_2O$ where M=Fe(III), Co(II), Ni(II), Cu(II), Zn(II) and Cd(II); A=Cl in case of Fe(III) and $x = 2$, in case of Fe(III), Co(II), Zn(II) and Cd(II), and 4, in case of Ni(II) and Cu(II).

The thermal analysis curve of Fe(III) complex of the general formula $[FeC_{30}H_{24}N_{10}O_4]Cl \cdot 2H_2O$ is shown in Fig. 1a. It gives pattern two stages of decomposition supported by DTA data (Table 2). The first step in the decomposition is started at

Table 3
Thermodynamic data of the thermal decomposition of BIAAP–metal complexes

Complex	Decomposition range (°C)	E^* (kJ mol^{-1})	A (S^{-1})	ΔS^* (JK^{-1} mol^{-1})	ΔH^* (kJ mol^{-1})	ΔG^* (kJ mol^{-1})
$[FeC_{30}H_{24}N_{10}O_4]Cl \cdot 2H_2O$	50–202	161.60	3.21×10^{14}	3.50	157.7	156.1
	202–665	43.68	8.83×10^{14}	−25.68	38.74	53.98
$[CoC_{30}H_{24}N_{10}O_4] \cdot 2H_2O$	50–205	37.39	2.75×10^5	−17.02	34.71	40.19
	205–650	27.39	2.75×10^5	−17.82	31.42	44.2
$[NiC_{30}H_{24}N_{10}O_4] \cdot 4H_2O$	50–185	148.4	5.61×10^{10}	−5.25	144.2	146.8
	185–565	190.1	2.28×10^{21}	−4.93	183.1	187.2
$[CuC_{30}H_{24}N_{10}O_4] \cdot 4H_2O$	50–205	34.00	5.82×10^3	−21.35	60.05	71.12
	205–770	112.4	1.67×10^4	−18.95	100.2	150.3
$[ZnC_{30}H_{24}N_{10}O_4] \cdot 2H_2O$	50–215	22.83	1.41×10^6	15.39	20.13	25.13
	215–460	91.00	1.07×10^{17}	−13.99	85.94	94.46
	460–955	89.02	7.12×10^3	−21.81	80.64	102.6
$[CdC_{30}H_{24}N_{10}O_4] \cdot 2H_2O$	50–190	106.9	3.96×10^{13}	1.56	103.6	102.9
	190–275	178.1	3.86×10^{16}	8.12	173.5	169.1
	275–490	123.3	1.42×10^9	−9.19	117.8	123.9
	490–1000	209.4	4.01×10^{13}	0.91	203.0	202.3

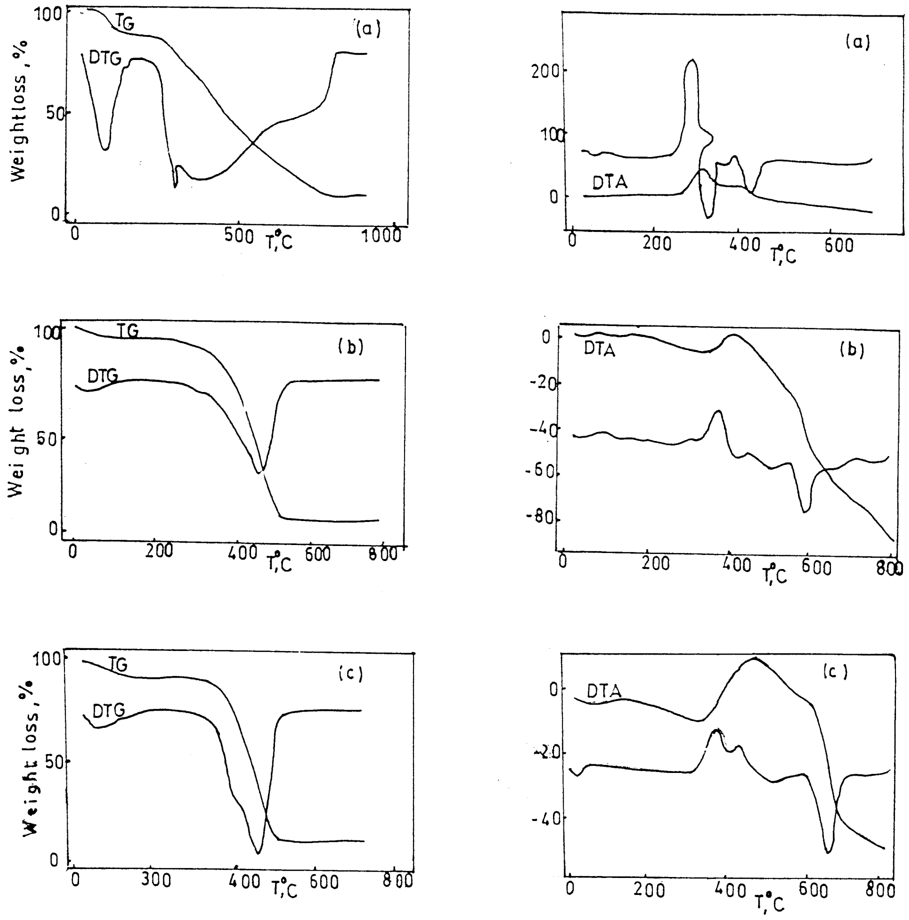

Fig. 1. Thermal analysis (TG and DTA) of BIAAP complexes: (a) Fe(III); (b) Co(II) and (c) Ni(II).

50–202 °C and corresponding to dehydration of the complex and loss of HCl gas with an estimated mass loss of 10.09% (calcd. mass loss 10.13%). This step is correlated with the endothermic peak in DTA at 60 °C. The energy of activation of the thermal dehydration of the complex was 161.57 kJ mol^{-1} (Table 3). In the second step, the decomposition of the two BIAAP molecules takes place in the temperature range 202–665 °C with an estimated mass loss 78.74% (calcd. mass loss 78.68%). This is confirmed by the presence of two endothermic peaks in the DTA at 330 and 480 °C and exothermic peak at 285 °C due to the liberation of the BIAAP molecules. The remainder was ferric hydroxide [M.wt = 107 (m/z = 106; RI. 34.59%)] as the product of decomposition which correlated with the mass spectra.

The cobalt complex of the formula $[CoC_{30}H_{24}N_{10}O_4]\cdot 2H_2O$ was thermally decomposed in two successive decomposition steps. The first estimated mass loss of 5.07% within the temperature range 50–205 °C with exotherm in the DTA at 90 °C, might be attributed to the liberation of two molecules of hydrated water (calcd. mass loss 5.27%). The energy of activation of this step is 37.39 kJ mol^{-1}. The second step occurs within the temperature range 205–650 °C with an estimated mass loss 83.72% (calcd. mass loss 84.04%) which is reasonably accounted for the decomposition of two ligand molecules leaving CoO residue. The appearance of exothermic peak at 360 °C and two successive endothermic peaks at 480 and 570 °C in the DTA curve (Fig. 1b) is related to the loss and fragmentation of two ligand molecules. The appearance of broad endothermic peak at 770 °C may be due to the phase transition occurs in the solid complex. The remaining CoO (M.wt = 75) was as a residue of the decomposition is confirmed by means of mass spectra [*m*/*z* = 75, RI. 23.94%].

Fig. 1c illustrates the thermal analyses curves of the Ni(II) complex with the general formula $[NiC_{30}H_{24}N_{10}O_4]\cdot 4H_2O$. The first estimated mass loss of 9.33% (calcd. mass loss 10.0%) at 50–185 °C with one small endothermic peak at 38 °C may be attributed to the thermal dehydration of the complex. The activation energy of dehydration is 148.4 kJ mol^{-1}. In the second step, within the temperature range 185–565 °C, the organic part of the anhydrous complex decomposed with an estimated mass loss 79.03% (calcd. mass loss 79.55%). Two successive exothermic peaks appear at 350 and 480 °C as shown in the DTA curve may be attributed to the decomposition of two BIAAP molecules. The appearance of strong endothermic peak at 610 °C may be reasonably related to phase transition. The remaining NiO (M.wt = 75) was confirmed by mass spectra (*m*/*z* = 76, RI. 17.95%).

On the other hand, Cu(II) complex of the formula $[CuC_{30}H_{24}N_{10}O_4]\cdot 4H_2O$ exhibits two distinct decomposition steps, as shown in Fig. 2d. The first step, in the temperature range 60–205 °C, with an estimated mass loss of 5.39% and two small exothermic peaks in the DTA may be attributed to the liberation of two molecules of hydrated water (calcd. mass loss 4.98%). The activation energy of the thermal dehydration of the complex is 64.36 kJ mol^{-1}. In the second step, DTA curve reveals an exothermic peak at 350 °C followed by three successive endothermic peaks at 430, 560 and 660 °C, respectively. This may be accounted to the vigorous decomposition of the BIAAP molecules leaving $CuCO_3$ as a metallic residue. The overall loss of mass from the thermogravimetric analysis (TG) curve is 82.50%, while the overall calculated mass loss is 82.93%. The remaining copper carbonate (M.wt = 123.5) was confirmed as the product of thermal decomposition by means of mass spectra (*m*/*z* = 123, RI. 59.06%).

The TG curve of the Zn(II) complex of the formula $[ZnC_{30}H_{24}N_{10}O_4]\cdot 2H_2O$ indicates that, the complex decomposed in three steps. The DTA curve of the complex shows one exothermic peak at 100 °C. This peak is assigned as the dehydration of the complex. This assignment was confirmed by the mass loss 7.49% at the temperature range of 50–215 °C (calcd. mass loss 7.55%) obtained from the TG curve. This corresponds to the loss of two water molecules and methane gas. It is found that, the activation energy of the dehydration step is equal to 22.83 kJ mol^{-1}. The second (215–460 °C) and third (460–955 °C) steps correspond to the removal of the two BIAAP molecules as deduced from mass loss calculations (estimated mass loss 87.19%, calcd. mass loss 88.25%). The appearance of endothermic peak in DTA at 280 °C followed by exothermic peak at 400 °C may be attributed to the strong vigorous chemical reaction of organic ligand molecule by loss of $C_7H_4NO_2$ leaving $[ZnC_{22}H_{16}N_9O_2]$ as stable compound as given in TG. Appearance of four successive endothermic peaks at 500, 600, 680 and 900 °C respectively may be related to further removal of the ligand molecule from Zn(II) ion and constant weight of ZnO has been formed which confirmed by mass spectra (*m*/*z* = 81.8; RI. 49.43%).

The Cd(II) complex, $[CdC_{30}H_{24}N_{10}O_4]\cdot 2H_2O$, exhibits four steps of decomposition on TG and eight peaks in DTA (Fig. 1f). The first endothermic peak at 130 °C corresponds to the loss of two water molecules and methane gas with an estimated mass loss 6.26% (calcd. mass loss 7.07%). It is found that the value of activation energy for this dehydration process is 106.9 kJ mol^{-1}. Several simultaneous decomposition processes with six successive endothermic and exothermic DTA peaks are observed between 193 and 1000 °C. The appearance of two endothermic peaks at 200 and 250 °C may referred to the liberation of CO and $2H_2$ gases. This is followed by another two successive endothermic peaks at 400 and 460 °C, which may be attributed to the vigorous chemical reaction and loss of $[C_7H_3N_3O]$ from ligand molecules and the rearrangement of complex configuration. This is followed by another two successive endothermic peaks followed by strongly exothermic peaks at 680, 800 and 920 °C, respectively, which may be attributed to the decomposition of residual part of ligand molecules and removal of [$C_{21}H_{31}N_7O_2$] and formation of CdO (M.wt = 128) as illustrated in TG and mass spectra ($m/z = 128$, RI = 10.62%).

In general, the stages of thermal decomposition of the complexes can be written as shown in Scheme 1. The estimated mass losses of the dehydration step are consistent with the calculated data (Table 2).

The anhydrous BIAAP complexes show great thermal stability up to 215 °C and in the second and subsequent stages, the decomposition and combustion of the BIAAP molecules in the complexes occur. The natures of the intermediates formed in the other subsequent steps are proposed and they give violent decomposition to give the respective metal oxides or carbonate as the final products. The formation of metal oxides or carbonate was confirmed by mass spectra.

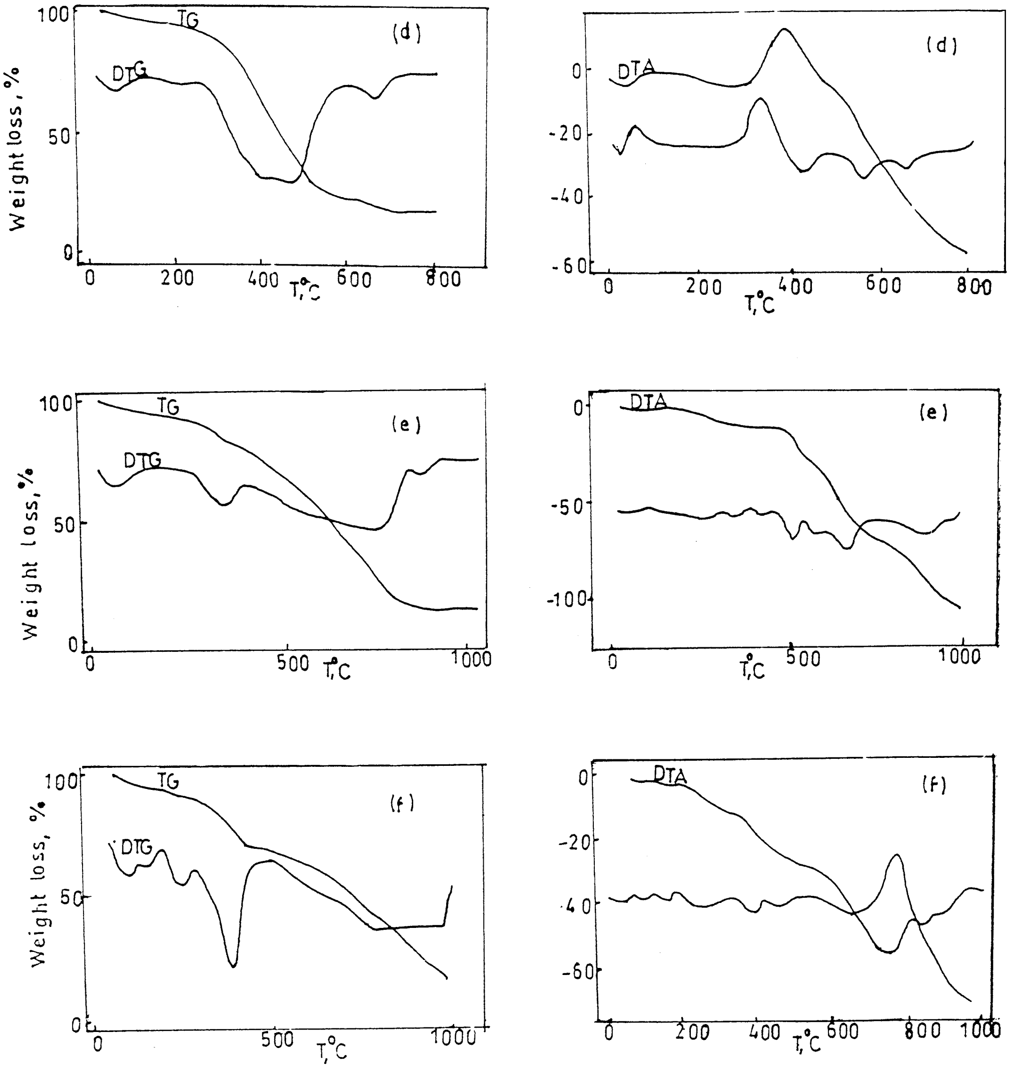

Fig. 2. Thermal analysis (TG and DTA) of BIAAP complexes: (d) Cu (II); (e) Zn (II) and (f) Cd (II).

$$[\mathrm{M(BIAAP)_2}]\,.x\mathrm{H_2O} \xrightarrow{50\text{-}205\ ^0\mathrm{C}} [\mathrm{M(BIAAP)_2}] + x\mathrm{H_2O}$$

$$[\mathrm{M(BIAAP)_2}] \xrightarrow{205\text{-}1000\ ^0\mathrm{C}} \mathrm{MO} + 2\ \mathrm{BIAAP}$$

where M = Co(II)(x = 2), Ni(II) (x = 4), Zn(II) (x = 2) and Cd(II) (x = 2).

For Cu(II) complex:

$$[\mathrm{Cu(BIAAP)_2}]\,.4\mathrm{H_2O} \xrightarrow{50\text{-}205\ ^0\mathrm{C}} [\mathrm{Cu(BIAAP)_2}]\,.2\mathrm{H_2O} + 2\mathrm{H_2O}$$

$$[\mathrm{Cu(BIAAP)_2}]\,.2\mathrm{H_2O} \xrightarrow{205\text{-}770\ ^0\mathrm{C}} \mathrm{CuCO_3} + 2\ \mathrm{BIAAP} + 2\mathrm{H_2O}$$

For Fe(III) complex:

$$[\mathrm{Fe(BIAAP)_2}]\mathrm{Cl}\,.2\mathrm{H_2O} \xrightarrow{50\text{-}202\ ^0\mathrm{C}} [\mathrm{Fe(BIAAP)_2}] + 2\mathrm{H_2O} + \mathrm{HCl}$$

$$[\mathrm{Fe(BIAAP)_2}] \xrightarrow{202\text{-}665\ ^0\mathrm{C}} 1/2\mathrm{Fe_2O_3} + 2\ \mathrm{BIAAP}$$

Scheme 1. General equations for the decomposition of BIAAP–metal complexes.

3.4. Relation between thermal stability of the hydrated complexes and initial temperature of decomposition

In order to check the thermal stability of complexes in the solid state, initial temperatures of the decomposition of the anhydrous complexes were compared. A plot of the initial decomposition temperatures of the anhydrous complexes and the corresponding reciprocal ionic radii of the di- and tri-valent metal ions against the atomic number is shown in (Fig. 3). The reciprocal of the ionic radii of the divalent metal ions decreases from Fe(III) to Co(II) with the decrease of initial temperatures of decomposition. While the reciprocal of the ionic radii increases from Co(II) to Ni(II) and the thermal stabilities of these complexes also increases. The same trend appears in comparing between the thermal stabilities and the reciprocal of ionic radii from Ni(II) to Cd(II) which decreases from Ni(II) to Cd(II). It is evident that the thermal stabilities of the complexes increase as the ionic radii decreased [15,16]. From the above results, it is qualitatively concluded that the thermal stability of the complexes follow the order Ni(II) > Cu(II) > Zn(II) > Fe(III) > Co(II) > Cd(II). The corresponding reciprocal ionic radii of the tri and divalent metal ions against the atomic number exhibit the same definite trend.

On the other hand Fig. 4 shows the change of E^* and ΔG^* with the increase of atomic number in the 3d- series of d-block elements, for the first decomposition step of their complexes with BIAAP. The complexes of $\mathrm{Fe^{3+}}$ (d^5), $\mathrm{Ni^{2+}}$ (d^8) and $\mathrm{Cd^{2+}}$ (d^9) with BIAAP are present on the top peaks of the energy curve. This means that these complexes are stable at the beginning of the decomposition than those on the bottom of the curve ($\mathrm{Co^{2+}}$ (d^7), $\mathrm{Cu^{2+}}$ (d^9) and $\mathrm{Zn^{2+}}$ (d^{10}) complexes). The same trend is gained for these complexes at the second step of decomposition, except they are become excited before going to decompose. These qualitative explanations of results mean also that the thermal stability is mainly related to the stereo-structure of the complexes and the electronic configuration of the d-block elements. Therefore, after calculation of

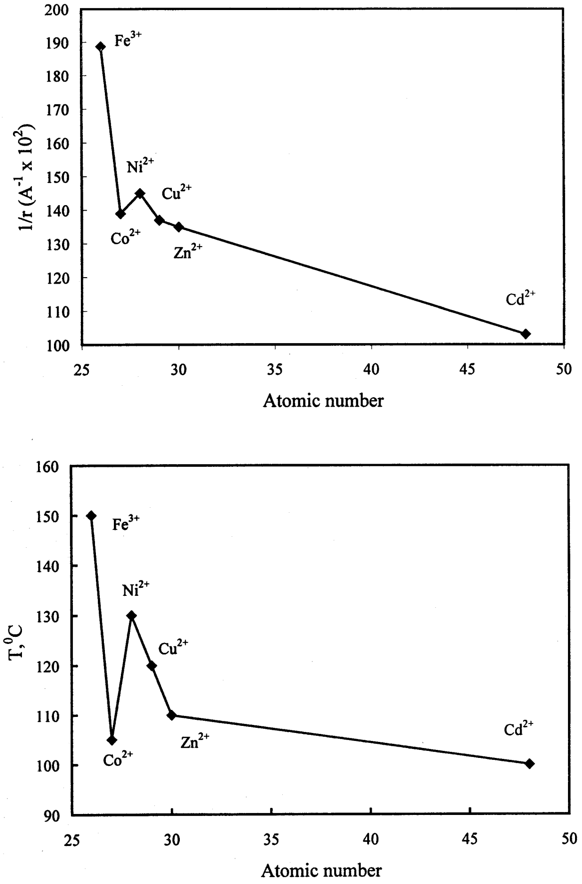

Fig. 3. Initial temprature of hydrated complexes and reciprocals of ionic radii of di- and tri-valent metal ions vs. atomic number.

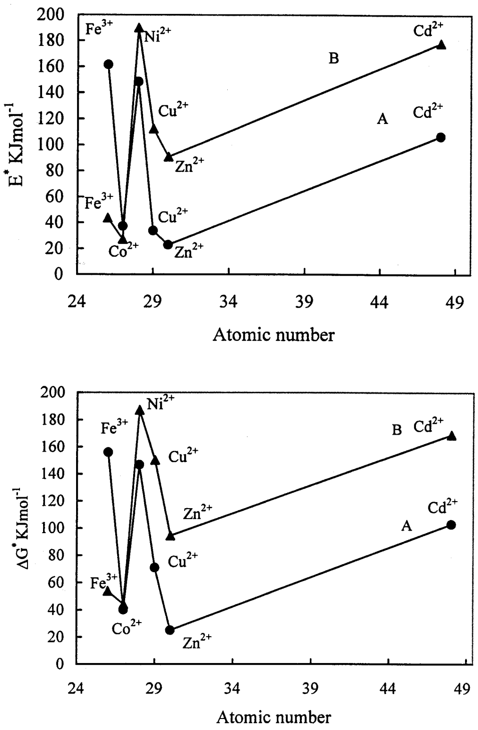

Fig. 4. Activation energy and free energy change of di-and trivalent metal ions complexes of BIAAP vs. atomic number: (A) at the first decomposition step; (B) at the second decomposition step.

pairing up energy P and energy of splitting of metal orbitals in octahedral Δ_0 and tetrahedral Δ_t in strong environment, those elements of Fe^{3+} (d^5) (t_2g^5 eg^0, $\Delta_0 = -10/12-P$), Ni^{2+}(d^8) (t_2g^6 eg^2, $\Delta_0 = -6/12-2P$) and Cd^{2+} (d^9) (t_2g^6 eg^3, $\Delta_t = -3/12$) are stable due to they have high pairing up energy. The other elements Co^{2+} (d^7) (t_2g^6 eg^1, $\Delta_0 = -9/12$), Cu^{2+} (d^9) (t_2g^6 eg^3, $\Delta_0 = -3/12-2P$) and Zn^{2+} (d^{10}) (t_2g^6 eg^4, $\Delta_t = 0$) have the less stability due to the less pairing effect. Fe^{3+} is present in the middle; Cd^{2+} is present in the top of the curve while Zn^{2+} is present at the bottom. This may be due to the fact that Fe^{3+} has a half filled orbital due to competition between splitting and pairing up effect and it's odd electron system while, Cd^{2+} may has completely filled d-orbital (d^{10}). The unusual behaviour of Cd^{2+} complex may be also attributed to strong bonding of the two BIAAP through their nitrogen and oxygen donor atoms to this metal ions which make the loss of these two ligands occurs in more than one step. It can be concluded that, the relation between E^* and ΔG^* vs. atomic number give a quantitative interpretation to the thermal stability of the complexes while the relation between the decomposition temperature and ($1/r$) vs. atomic number give a qualitative assignment. Also, the kinetic data (Table 3) shows that, all the complexes have −ve entropy which indicates that activated complexes have more ordered systems than reactants.

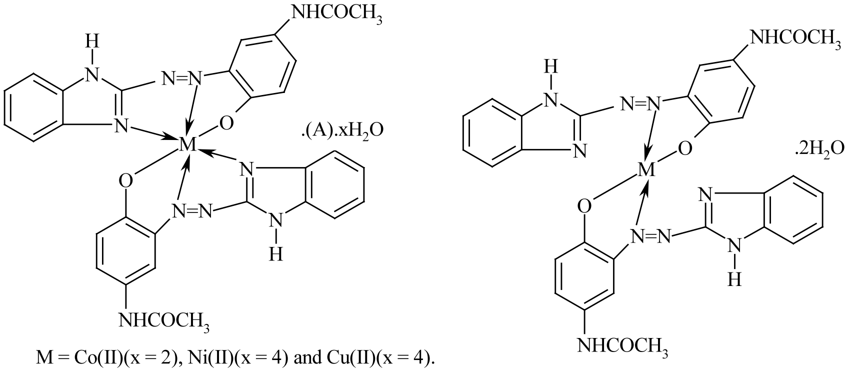

M = Co(II)(x = 2), Ni(II)(x = 4) and Cu(II)(x = 4).
= Fe(III), A = Cl, x = 2.

M = Zn(II) and Cd(II)

Fig. 5. Proposed structural formulas of BIAAP–metal complexes.

4. Conclusion

As a general conclusion, the BIAAP ligand behaves as a monobasic ligand in 1:2 complex with tridentate ONN donors derived from the phenolic oxygen, α N of the azo group forming a two binding chelating sites. In octahedral complexes, the two extra positions are provided by the pyridine like nitrogen of the imidazole moiety. The proposed general structures are shown in Fig. 5. The thermal stabilities of the complexes increase as the ionic radii decrease [15,16]. From the above results, it is quantitatively concluded that, the thermal stability of the complexes follows the order Ni(II) > Cu(II) > Zn(II) > Fe(III) > Co(II) > Cd(II). The corresponding reciprocal ionic radii of the di- and tri-valent metal ions against the atomic number exhibit the same definite trends.

References

[1] J.C. Agroud, C. Disant, R. Massot, A. Cornu, Bull. Inf. Sci. Tech. Commis. Energ. At. 230 (1979) 203.

[2] Y. Ihara, R. Tsuchiya, Bull. Chem. Soc. Jpn 53 (1980) 1614.

[3] D.A. Garnovskii, A.S. Antsyshkina, A.P. Sadimenko, M.A. Porai-Koshits, O.A. Osipov, A.D. Garnovskii, Dokl. Akad. Nauk. SSSR 296 (1987) 1119.

[4] M. Cristina, A. Jose Garcia, J.R. Masaguer, Transition Met. Chem. 12 (1987) 249.

[5] B. Lenarcik, J. Glowacki, M. Gabryszewski, R. Czopek, Pol. J. Chem. 64 (1990) 43.

[6] A. Arquero, P. Souza, J.A. Garcia-Vazquez, J.R. Masaguer, Transition Met. Chem. 10 (1985) 424.

[7] P. Souza, J.A. Garcia-Vazquez, J.R. Masaguer, Transition Met. Chem. 9 (1984) 318.

[8] M.A. Meudiola, J.R. Masaguer, C. Molleda, Synth. React. Inorg. Met.-Org. Chem. 22 (1992) 955.

[9] A.W. Coats, J.P. Redfern, Nature 201 (1964) 64.

[10] J.J. Fiol, A. Terron, D. Mulet, V. Merno, Inorg. Chim. Acta 135 (1987) 197.

[11] Z.M. Zaki, S.S. Haggag, A.A. Soayed, Spectrosc. Lett. 31 (1998) 757.

[12] P.M. Drozdzewski, Spectrochim. Acta 44A (1988) 1297.

[13] M.S. Nair, M.A. Neelakantan, S.S. Sunu, Theor. Anal. Chem. 38A (1999) 1307.

[14] G.G. Mohamed, Nadia E. El-Gamel, F.A. Nour El-Dien, Synth. React. Inorg. Met.-Org. Chem. 31 (2) (2001) 347–358.

[15] G.G. Mohamed, F.A. Nour El-Dien, N.E.A. El-Gamel, J. Thermal Anal. Calorimetry 67 (2002) 135–146.

[16] H. Icbudak, V.T. Yilmaz, H. Olmez, J. Thermal Analy. 53 (1998) 843.